AUT Journal of Modeling and Simulation

AUT J. Model. Simul., 56(1) (2024) 55-68
DOI: 10.22060/miscj.2024.22964.5353

Novel Design of Optically Transparent Circuit Analog Absorber by Modifying of exponentially tapered edge of element to achieve wider Bandwidth

Reza Mirzakhani *, Alireza Bayat

Faculty of Technical and Engineering, Electrical Engineering-Telecommunication, Imam Khomeini International University of Qazvin, Iran.

ABSTRACT: This paper presents a novel design and analysis of a single-layer, exponentially tapered circuit analogue absorber (CAA) that is flexible and optically transparent. By modifying the edge of conventional crossed strips to an exponential taper, a wider bandwidth is achieved, analysed through current distribution and on the top layer of the unit cell. The designed unit cell comprises of ITO-Coated-PET a ground plane and CA absorber layer and a quarter-wavelength PVC dielectric substrate, achieving over 80% transparency and a relative bandwidth exceeding 85%. Comparative analysis with Numerical and experimental results and conventional CAA unit cells is conducted. Also, the current distribution is expressed mathematically. Parametric studies investigate various design parameters and CA elements to enhance impedance matching and absorption properties across the 2 to 25 GHz frequency range. Challenges such as the impact of layer count, substrate thickness, and analogue element type on transparency and absorption are mitigated by optimizing absorber dimensions and employing tapered shapes for strips to widen the bandwidth. This innovative CAA design finds applications in electromagnetic compatibility, radar cross-section reduction, offering a balance between wide bandwidth electromagnetic shielding and absorbing and high optical transparency, suitable for aircraft windshields, fighter canopies, space station windows end etc.

Review History:

Received: Feb. 02, 2024
Revised: May, 02, 2024
Accepted: Jun. 21, 2024
Available Online: Sep. 05, 2024

Keywords:

Circuit Analog Absorber
Indium Tin-Oxide
Bandwidth
Shielding Effectiveness
Current Distribution

1- Introduction

The circuit analogue absorber (CAA) is a type of electromagnetic absorber that uses a periodic structure of circuit analogue to achieve high absorption performance [1]. The CAA also is a kind of nonmagnetic planar absorber, which consists of sheets of periodic planar frequency selective surfaces (FSS) [2]. The term circuit analogue for such absorbers is derived from the fact that the geometrical patterns are often defined in terms of the effective resistance, capacitance, and inductance. Equivalent circuit techniques are then used in the subsequent analysis and design of the resulting absorber [3]. As you see in Figure 1 [1], The structure consists of a ground plane and a circuit analogue sheet separated by a quarter-wavelength dielectric substrate. The circuit analogue sheet is made up of two perpendicular cross strips, which can be constructed using one or several layers. The CAAs are an improved version of Salisbury screen radar absorbers that introduce FSS instead of a resistive sheet with free-space impedance [4]. The absorber is designed to work over a wide range of frequencies and has been shown to have excellent absorption properties, particularly in microwave and millimetre-wave frequency ranges.

In the first type, the orthogonal cross strips are positioned on two opposite sides of a dielectric substrate, and the current is distributed uniformly throughout the strips. In the second type, each of the two strips is placed on one side of the dielectric substrate, and they are made of the same homogeneous strip. In this case, not only is the current distribution non-uniform, but the distribution in the intersection areas of the two strips is also different. This phenomenon can be attributed to the fringing effect observed in the parallel plates of a capacitor [5]. The current distribution in both types has been studied extensively, and formulas have been derived [1].

Several design parameters, such as the dimensions and spacing of the circuit analogue elements, have been investigated to achieve better impedance matching and higher absorption. Additionally, different types of circuit analogue elements, including the Jerusalem cross, E-shaped patch, and meander line, have been used to construct the absorber [1] [3] [5] [6] [7] [8].

The CAA has numerous applications in areas such as electromagnetic compatibility, radar cross-section reduction, and antenna design. It offers several advantages over other types of absorbers, including its wide bandwidth, low profile, and ease of fabrication. However, its performance can be affected by factors such as the number of layers used in its construction, the thickness of the dielectric substrate, and the type of circuit analogue elements used [1] [3] [5] [6] [7].

To avoid the use of fat or bulky elements, these structures

*Corresponding author's email: reza.mirzakhani@edu.ikiu.ac.ir

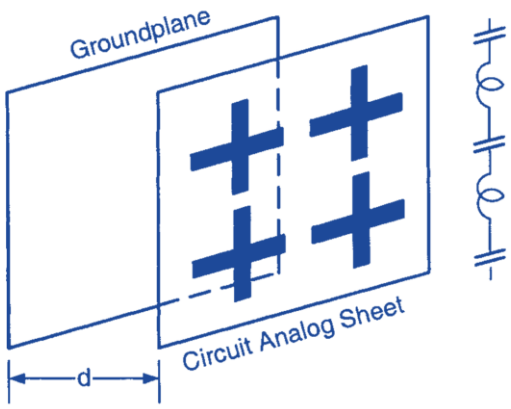

Fig. 1. Circuit Analog Absorber and Equivalent Circuit [1]

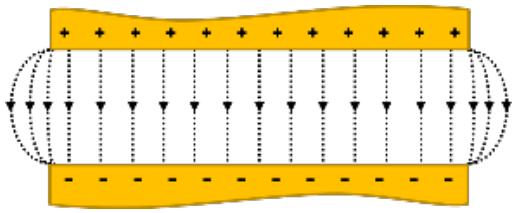

Fig. 2. The Fringing Effect Observed in The Parallel Plates of Capacitor

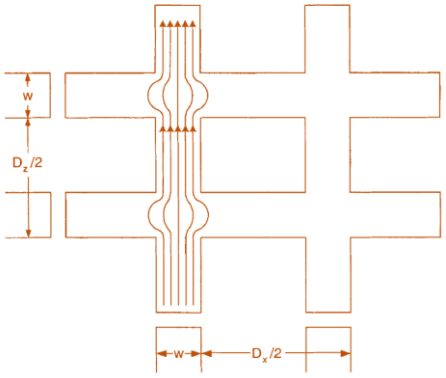

Fig. 3. The Fringing Effect Between Two Electrodes of Finite and Equal Length.

typically consist of thin and periodic patterns of conductive and dielectric materials that are designed to selectively reflect, absorb or transmit electromagnetic waves within a specific frequency range. By using such structures, it is possible to achieve high electromagnetic shielding effectiveness without significantly affecting optical visibility. The use of thin elements in such structures helps to reduce the overall thickness of the absorber and enhance its transparency, making it suitable for applications where optical visibility is critical. Fat elements, on the other hand, can make the structure more complex and bulkier, which may not be desirable for some applications [1].

On the other hand, the use of transparent electromagnetic shields has increased and has been widely used in various industrial, medical, and military applications. One of the best materials for transparent conductive shields is indium tin oxide, which is widely used due to its many features, including high optical transparency and good conductivity [9]. However, it is challenging to achieve both wide bandwidth electromagnetic shielding and high optical transparency. As the thickness of the electromagnetic shield increases, the optical transparency decreases, and vice versa.

1- 1- The Fringing Effect

The fringing effect on orthogonal cross strips in circuit analogue absorbers can lead to a non-uniform current distribution and a reduction in absorption efficiency. According to Weber [5], the fringing effect observed in the parallel plates of a capacitor (see Figure 2) can cause the current distribution to be non-uniform, and the distribution in the intersection areas of the two strips is also different. Weber explains that this is due to fringing on both sides of the capacitor, which can be considered as two semi-infinite cases in parallel where the plate width equals one-half of the

plate separation. Each of these semi-infinite cases has a 60% increase in flux due to fringing, which in turn means that the total resistance of the square common to the area of two crossing strips is reduced.

To mitigate the effects of fringing, various techniques have been proposed, including the use of periodic structures and the optimization of the dimensions of the circuit analogue absorber for better impedance matching. Thus, if the orthogonal strips cross each other n_c times within a strip length $2l_1$ (see Figure 3), the load resistance should be explained by $R_L^{'}$ [1].

$$R_L' = 2R_s l_1/3w\left[1 + 2C_1 - 1.1\,{}^{wn_c}/_{2l_1}\right] \text{(ohm)} \quad (1)$$

This effect is modelled mathematically using the concept of edge capacitance. The edge capacitance can be calculated using the following equation [9]:

$$C_{edge} = \left(\gamma . h_L^{\delta}\right).d.H(d - d_0) \quad (2)$$

Where , δ , and d_0 are the three fitting parameters and H(d-do) is the Helmholtz step function.

2- Theory and Design

2- 1- Periodic Structure

Periodic structures are a type of electromagnetic structures that have a repeating pattern at regular intervals. In radar absorbent structures (RAS), periodic structures are commonly used as the absorbing layer, because they can effectively attenuate the incident electromagnetic waves over a wide frequency range. An infinite array of metallic plates or strips forms a useful model for the analysis of many practical microwave structures. A more general formulation of the scattering problem of a two-dimensional periodic array of plates is studied by Chen in [10]. The periodicity of the structure plays a critical role in determining the electromagnetic properties of the RAS, such as the absorption bandwidth and polarization sensitivity. The periodic structure can be designed using a variety of methods, including fractal geometry, metamaterials, and photonic crystals.

2- 2- Properties of ITO

ITO is a transparent conductive material that is commonly used as a thin coating on PET films for various applications. PET is a type of plastic film that is widely used for packaging, displays, touchscreens, and other electronic devices. When PET films are coated with a thin layer of ITO, they gain properties such as high optical transparency and electrical conductivity. The combination of PET and ITO coating allows for the creation of flexible, transparent conductive films. These films are often used as transparent electrodes in electronic devices, including touchscreens, liquid crystal displays (LCDs), organic light-emitting diode (OLED) displays, solar cells, and electrochromic windows.

ITO-coated PET films provide excellent electrical conductivity while maintaining high light transmission, making them suitable for applications where both transparency and conductivity are required. However, it's worth noting that indium is a relatively rare and expensive element, which can contribute to the cost of ITO-coated PET films. Alternative transparent conductive materials, such as graphene and silver nanowires, are being explored as potential replacements for ITO due to their improved flexibility, durability, and cost-effectiveness. Nonetheless, ITO-coated PET remains a widely used and established technology in various industries.

E. A. Alwan et al [11] have conducted measurements to determine the electrical properties of ITO, specifically the permittivity and conductivity, over a frequency range of 0.1-20 GHz. As far as our knowledge goes, these measurements represent the first reported electrical properties of ITO across such a wideband range. The exact value of permittivity and conductivity could be calculated by using the following formula [11];

$$\sigma_{ITO}(\omega) = \frac{1}{t_{ITO} z_0}\,\mathrm{Re}\left\{\sqrt{\varepsilon_r}\,\frac{1-\Gamma_A}{1+\Gamma_A}\right\}\left(\frac{S}{m}\right) \quad (3)$$

$$\varepsilon_{r,ITO}(\omega) = \frac{\varepsilon'_{ITO} - {}^{j\sigma_{ITO}}/_{\omega}}{\varepsilon_0} \quad (4)$$

2- 3- Floquet Theorem

The Floquet port method is a numerical technique used to analyse the electromagnetic behaviour of periodic structures, such as frequency-selective surfaces or photonic crystals. The method is based on the Floquet theorem [12], which states that the solution to Maxwell's equations for a periodic structure can be expressed as a linear combination of plane waves with specific wave vectors. In the Floquet port method, the periodic structure is divided into a unit cell and the boundary conditions at the edges of the cell are expressed in terms of the Floquet modes. The Floquet port method allows the calculation of the scattering parameters of the periodic structure, which describes how the structure interacts with incident electromagnetic waves. Overall, the Floquet port method is a powerful and widely used technique for the design and analysis of periodic structures in electromagnetics [13]. The Floquet modes can be written as [14]:

If E(t) is a fundamental matrix solution (such as an electric field) of the T -periodic system, then, for all t ∈ R,

$$E(t + T) = E(t)E^{-1}(0)E(T) \quad (5)$$

In addition, there is a matrix B (which may be complex) such that $e^{TB} = E^{-1}(0)E(T)$ and a T -periodic matrix function t → P (t) (which may be complex-valued) such that

$E(t) = P(t)e^{tB}$ for all t ∈ R. Also, there is a real matrix R and a real 2T -periodic matrix function t → Q(t) such that $Q(t)e^{tR}$ for all t ∈ R [14]. where E is the electric field, t is the position along the direction of periodicity, and T is the period of the structure.

Using the Floquet modes, the boundary conditions at the edges of the unit cell can be expressed in terms of the scattering matrices [15]. The scattering matrices relate the incident and reflected waves at the input and output ports of the unit cell to the electric and magnetic fields inside the cell. The overall scattering from the structure is determined by first evaluating a matrix of scattering parameters for each individual layer and then forming a scattering matrix for the entire structure by a procedure analogous to the cascading of networks in circuit theory [16]. The scattering matrices can be written as:

$$[S] = [A]e^{-J\beta T} \quad (6)$$

where [S] is the scattering matrix, [A] is the amplitude matrix, β is the propagation constant, and T is the period of the structure. The scattering parameters describe how the structure interacts with incident electromagnetic waves and can be used to optimize the design of the structure. The procedure to be presented here is to expand the electromagnetic field distribution near the array of the conducting plates into a set of Floquet mode functions. By requiring the total electric field to vanish on the conducting plates, an integral equation for the unknown current on each plate is obtained. The electromagnetic fields must satisfy the periodicity requirements imposed by Floquet's theorem [10].

You can construct unit cells for frequency selective surface (FSS) simulations using linked boundaries and two Floquet ports, with one port above the plane of the structure and the other port under it. The applied excitations are the Floquet modes themselves, usually one or both specular modes. As a direct result of the field solution, the reflection and transmission properties of the FSS are cast in terms of the computed S-matrix entries interrelating the Floquet modes. In CST Studio [17], Floquet ports calculate the resulting fields within the structure.

The Floquet port relation for FSS is a mathematical expression that relates the electric and magnetic fields at the edges of the unit cell of the FSS. The relation is based on the periodicity of the FSS and the concept of Bloch's theorem [18], which states that the electric and magnetic fields in a periodic structure can be represented by a combination of a plane wave and a phase factor. The Floquet port relation for an FSS cell in CST Studio can be expressed as [E, H] = [T] * [E', H'] [17]. Where [E, H] is the electric and magnetic fields at the edges of the FSS cell, [E', H'] is the electric and magnetic fields at the virtual Floquet port, and [T] is the transfer matrix that relates the fields at the edges of the cell to those at the Floquet port. The transfer matrix is calculated based on the geometry of the FSS cell, the substrate properties, and the excitation wavelength. The accuracy depends upon the number of modes used to approximate the induced current on each plate and the number of Floquet modes used to approximate the near field of distribution [10].

The plane wave expansion in Floquet mode is a technique used in the analysis of periodic structures, particularly in the context of electromagnetics and photonics. This method leverages the periodicity of the structure to simplify the problem by expanding the fields into a series of plane waves, each modulated by a periodic function known as the Floquet mode. In the plane wave expansion method, the electromagnetic fields are expanded into a series of plane waves. Each plane wave corresponds to a specific wave vector, and the fields are represented as:

$$E(r) = \sum_G E_G e^{j(K+G).r} \quad (7)$$

Where G is a reciprocal lattice vector of the periodic structure, E_G is the amplitude of the plane wave with wavevector (K+G). If this structure is exposed to an incident plane wave propagating in the direction of then the amplitude of all the element currents will be the same, while their phases will match the phase of the incident field. Put formally, for the element current in column q and row m is;

$$\hat{S} = \hat{X}S_x + \hat{Y}S_y + \hat{Z}S_z \quad (8)$$

$$I_{qm} = I_{o,o}e^{-j\beta qD_x S_x}e^{-j\beta mD_z S_z} \quad (9)$$

As in the single infinite vase above, this is a direct consequence of the floquet theorem [1].

2- 4- Analysis of Exponential Taper and impedance matching

Tapered shapes can be used for the strip in the CAA to improve the bandwidth of the absorber. By gradually tapering the edges of the strip, the electromagnetic energy can be more effectively coupled into the absorber layer, which leads to a wider absorption bandwidth. The tapering can be achieved by changing the width or depth of the strip gradually from the centre to the edges of the unit cell. Several studies have investigated the use of tapered shapes for the strip in the CAA. The results showed that the tapered slots led to a significant improvement in the bandwidth of the absorber. Burleson examines the use of tapered periodic two-dimensional edge treatments to reduce wide-band edge diffraction from a knife edge for the polarization parallel to the plane of incidence [19]**.** There are mathematical analysis models that can be used to design tapered strips for circuit analogue absorbers. The analysis involves determining the resonance frequency

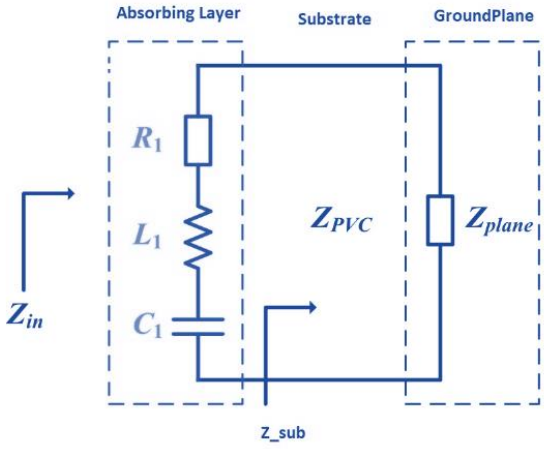

Fig. 4. Equivalent Circuit Model of Single Layer Absorber

of the tapered strip and the corresponding absorption bandwidth. One commonly used model is the transmission line model [20], which considers the strip as a short-circuited transmission line. The width and length of the strip, as well as the taper angle and the spacing between adjacent strips, can be optimized to achieve the desired absorption performance. The model takes into account the inductive and capacitive effects of the slot and the surrounding dielectric material.

Another model that can be used is the equivalent circuit model (refer to Figure 4), which represents the absorber as a network of lumped elements such as resistors, capacitors, and inductors. The values of these elements can be calculated based on the physical dimensions and material properties of the absorber, as well as the desired absorption bandwidth and level. Both of these models require some knowledge of electromagnetic theory and circuit analysis, as well as access to simulation software such as CST Microwave Studio [17]. Overall, both approaches can be used to design and optimize tapered slot shapes in absorbers to achieve wider bandwidths and improved absorption performance.

$$z_{sub} = Z_{pvc}\frac{Z_{plane}+jZ_{pvc}\tan(\beta d_{sub})}{Z_{pvc}+jZ_{plane}\tan(\beta d_{sub})} \tag{10}$$

$$z_{in} = \frac{1}{\frac{1}{z_{AL}}+\frac{1}{z_{sub}}} = \frac{Z_{AL}Z_{sub}}{Z_{AL}+Z_{sub}} \tag{11}$$

$$Z_{AL} = R + j\left(\omega L - \frac{1}{\omega C}\right) \tag{12}$$

$$Z_{plane} = jZ_m^{TE,TM}\tan(\beta d) \tag{13}$$

$$\Gamma = \frac{Z_{in}-Z_0}{Z_{in}+Z_o} \tag{14}$$

To find the relation between the width of orthogonal cross strips on CAA and the exponentially tapered edge of the strip from the centre to the edge of the cell, we need to determine the required values of absorbing layer impedance based on the desired tapering shape of the edge.

Tapered impedance transformers match an impedance Z_S to an impedance Z_L using a transmission line having a characteristic impedance Z_0 that gradually varies from Z_S to Z_L along the length of the line. The exponential taper has an exponential taper of the line's characteristic impedance. Setting $Z_0(z) = Z_x e^{az}$ with $a = \frac{1}{l}\ln\left(\frac{z_L}{z_S}\right)$ and $z_x = z_s e^{-al/2}$ results in the input reflection coefficient, derived using the Equation;

$$\Gamma_{in}(l) = \frac{1}{2}Z_x e^{-j\beta l}\int_{-\frac{l}{2}}^{\frac{l}{2}} e^{-2j\beta z}\frac{d\ln(e^{az})}{dz}dz = \frac{1}{2}\ln\left(\frac{Z_l}{Z_s}\right)\frac{(\sin(\beta l))}{\beta l} \tag{15}$$

So Γ_{in} has a sinc function characteristic with the variations of Γ_{in} reducing as the taper becomes longer. The main problem with this taper comes from the abrupt impedance

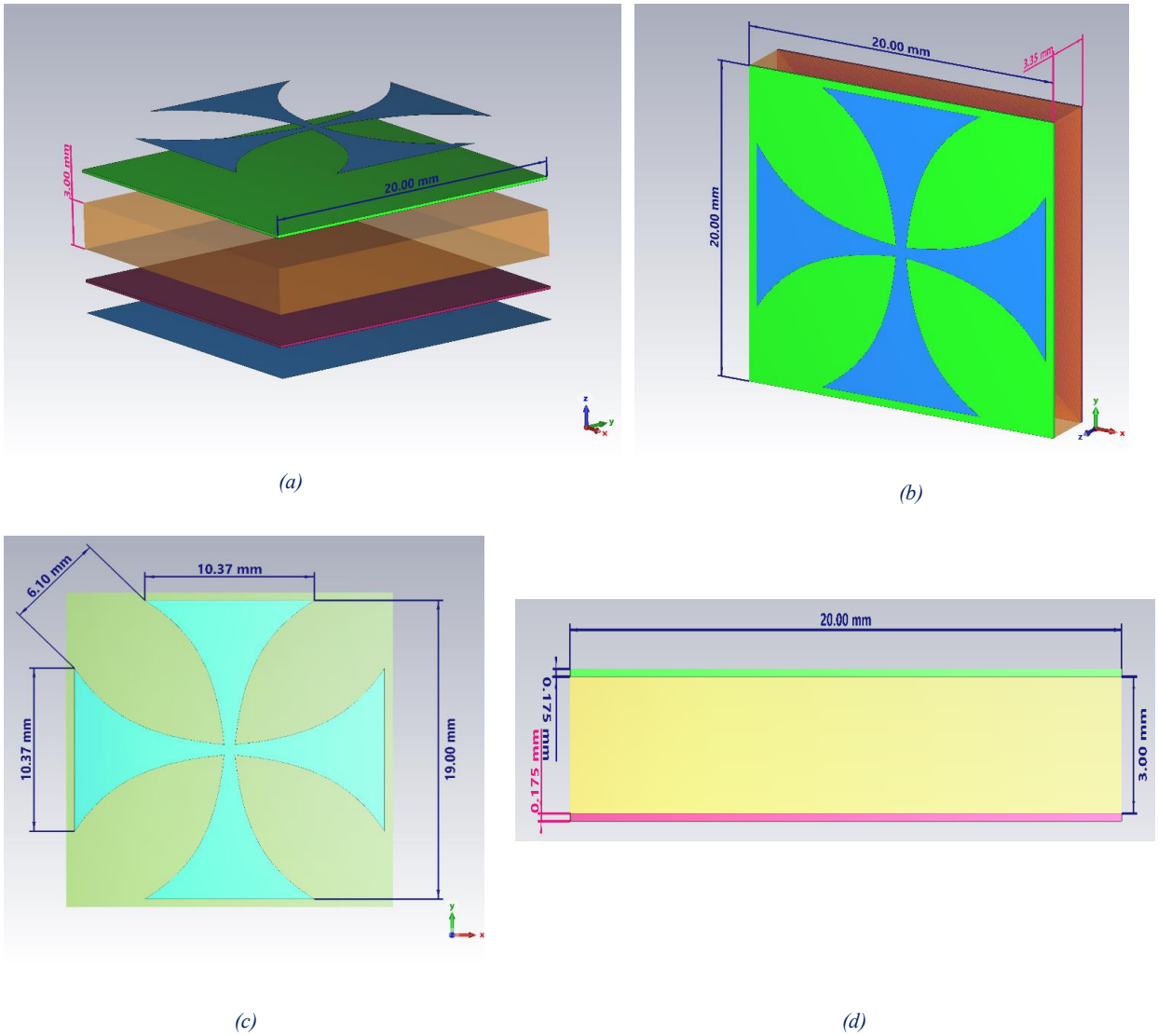

(a) *(b)*

(c) *(d)*

Fig. 5. (a)Explosive perspective view of unit cell (b) Perspective view of unit cell (c) Top View. (d) Side View. All the dimension are in mm.

discontinuity at the Z_1 end of the taper. [21]

3- Unit Cell Design and Simulation

3- 1- Unit Cell design

The proposed unit cell is shown in Figure 5(a) and consists of three optically transparent layers. The geometry parameters are presented in Figure and W is the overall width of a square patch with the dimension of $20\times20mm^2$ along the X-Y direction. it is consisting of the ground plane, substrate and absorber layer.

The substrate is made from Polyvinyl chloride (PVC) with the relative dielectric constant $\varepsilon_{PVC}=2.4(1-j\,0.06)$ that means the loss tangent of 0.06 and thickness of $d_{sub}=3mm$.

The Ground plane is a thin film of PET that is coated by a thin layer of indium tin oxide (ITO) with a surface resistance of $8\Omega/sq$. The relative dielectric constant of ITO-Coated-Pet is $\varepsilon_{PET}=3.0(1-j\,0.006)$ that means the loss tangent of 0.006 and thickness of $d_{sub}=0.175mm$.

The Circuit Analog Absorber is a thin film of PET that is coated by a thin layer of indium tin oxide (ITO) with a surface resistance of $8\Omega/sq$. The relative dielectric constant of ITO-Coated-Pet is $\varepsilon_{PET}=3.0(1-j\,0.006)$ that means the loss tangent of 0.006 and thickness of $d_{sub}=0.175mm$. Instead of using a crossed strip, the edge of the cross is tapered exponentially to gradually load the absorber element electrically to achieve wider bandwidth [22].

$$y=\pm S\times e^{r\times(t-B)}+C \tag{16}$$

Where s, r, and t stand for Cartesian exponential function parameters could be plotted in the parametric equation in 3D as a u(t), v(t) and w(t). Also “S” is the scaling factor, “r” is the exponential rate, B is the shifting value, and C the offset value [22].

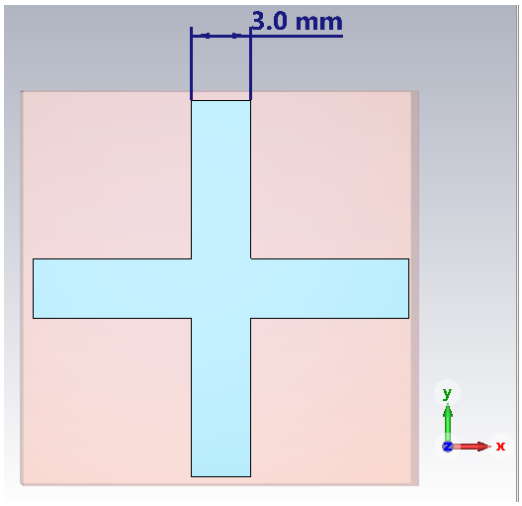

Fig. 6. Top View of Conventional Circuit Analog Absorber Unit Cell Simulated with CST Studio

3- 2- Simulation Results

In this study, we propose to employ numerical simulation techniques using CST Studio to modify conventional CAA with cross orthogonal cross strip to the exponentially tapered crossed strip to enhance bandwidth. Due to the singularity of the current distribution at the edges of a perfectly conducting strip, the convergence of the iteration process is much slower than for the resistive strips. By evaluating the boundary conditions using the least square error criterion, a rapid convergence can be assured when the cross-polarized field component is negligible [23]. If instead of a perfect conductor, we consider using indium tin oxide (ITO-Coated-PET) film, several changes and considerations come into play:

1. Convergence Rate: The convergence rate of the iteration process may be different compared to a perfect conductor. The presence of the ITO coating introduces additional complexities due to its conductivity and thickness. The singularity at the edges may still affect the convergence, but the specific behaviour would depend on the properties of the ITO film.

2. Boundary Conditions: The evaluation of boundary conditions using the least square error criterion can still be employed to enhance convergence. However, the specific boundary conditions would need to be adapted to the properties of the ITO coating and its interaction with the PET film.

3. Cross-Polarized Field Component: Neglecting the cross-polarized field component may still be applicable depending on the specific characteristics of the ITO-coated PET film. The assumption of negligible cross-polarized field components should be validated considering the electrical properties and geometry of the ITO film.

4. Electrical Properties: The conductivity of the ITO film plays a significant role in the current distribution. The electrical properties of ITO, such as sheet resistance and conductivity, would need to be incorporated into the analysis to accurately model the behaviour of the film.

5. Thickness Considerations: The thickness of the ITO coating on the PET film also affects the current distribution. Thicker coatings may have a more significant impact on the convergence rate and the overall behaviour of the system.

6. Material Modelling: The properties of the ITO-coated PET film would need to be accurately modelled and incorporated into the analysis. This includes considering the frequency-dependent behaviour, dispersion, and anisotropy of the ITO film.

For this purpose, the comparison is performed to ensure the achieved results. Figure 6 presents the conventional circuit analogue absorber unit cell. In this unit cell, the ITO-Coated-PET with the thickness of 0.175 mm is used as a ground plane and top CA absorber layer.

A parametric study was conducted to investigate the effect of varying the width of an orthogonal crossed strip in the range of 0.4 mm to 5 mm, with different step sizes. The scattering parameter results are presented in Figure 7. It was observed that different values were obtained for each dimension considered during the study. The best results were achieved at a resonant frequency of 18.6 GHz with a level of -24.38 dB. Notably, it was found that increasing the width of the crossed strip resulted in a shift in the resonant frequency. When the width of the crossed strip is increased, the fringing electric fields at the edges of the strip become more pronounced. The increased fringing effect leads to an increase in the effective capacitance of the unit cell. As a result, the resonant frequency decreases, causing a shift toward lower frequencies. Conversely, if the width of the crossed strip is

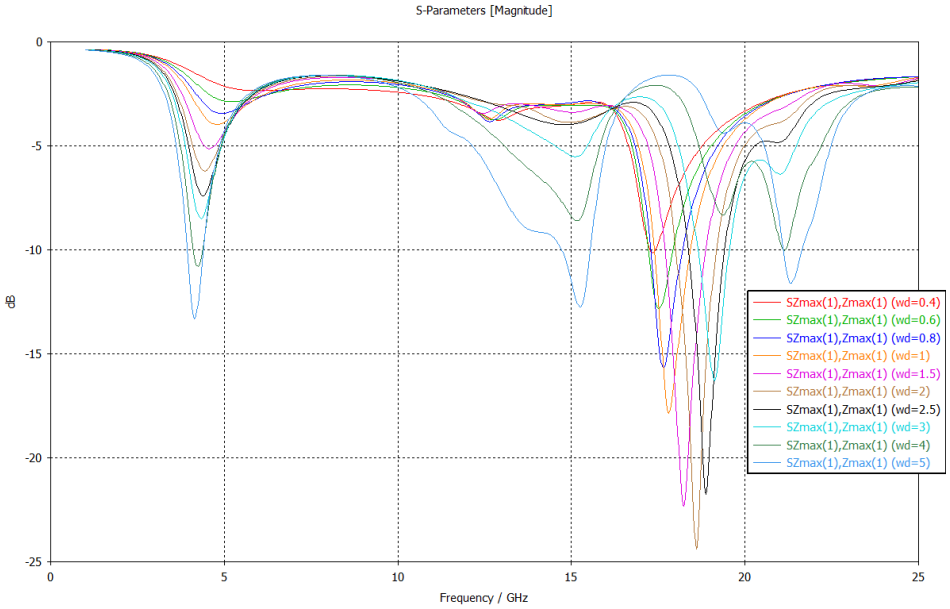

Fig. 7. Parametric Study of CAA: The Scattering Parameter Shows Variation with Regards to Parameter Wd ;sweep From 0.4 to 5 mm with 0.2 mm Step

reduced, the fringing effect becomes less significant, resulting in a decrease in the effective capacitance and a shift of the resonant frequency towards higher frequencies.

Also, the numerical analysis has been performed to find the scattering parameters of exponentially modified CAA. The simulation with a unit cell is illustrated in Figure 6 where the conventional crossed strip CAA is converted to the new design. In this method, 2 elements are intercepted at the center. So the transmission coefficient is yielded as a Figure 8 it shows that when the strips are connected at the center between frequencies of 0 to 25 GHz the scattering parameters at the resonant frequency of 15.327 GHz where the level is reached to -42.67 dB absorption. Also, the bandwidth is increased from 1.19 Ghz to 6.5 Ghz approximately.

To achieve the desired objectives, a comprehensive parametric study was conducted, focusing on varying the exponential parameters. This study explored the response corresponding to the exponential rate (r) through a carefully designed experimental setup, which involved three distinct steps. The obtained results from this investigation are presented in Figure 9, providing a visual representation of the observed response to the varying exponential rate. When the exponential rate "r" in the tapered edge configuration of the crossed strip in a CAA unit cell is increased or decreased, it influences the behaviour and performance of the absorber. The decrease in the exponential rate "r" tends to result in a reduction of the bandwidth of the absorber, while an increase in "r" generally leads to an enhancement of the absorber bandwidth. However, it is important to note that adjusting the value of "r" is a trade-off that affects other parameters as well. Decreasing "r" may limit the absorber's ability to effectively absorb a wide range of frequencies, resulting in a narrower bandwidth. On the other hand, increasing "r" can broaden the absorber's bandwidth, allowing it to absorb a wider range of frequencies.

However, it's crucial to consider the overall design objectives and constraints. Modifying "r" should be done in conjunction with other parameters and design considerations to ensure that desired performance characteristics are met. These parameters may include the dimensions of the absorber, the specific materials used, and the targeted frequency range. Therefore, while adjusting "r" can have a direct impact on the absorber's bandwidth, it is essential to carefully evaluate and optimize the interplay between "r" and other parameters to achieve the desired trade-off for the specific application.

Here are table number 1 where contains the comparison review with the previous research that constraint only with PET and PVC substrate;

Our study diverges from [24], [25], and [26] in several key aspects. Specifically, we utilize a single-layer structure with an overall thickness of 3.35 mm. This thin profile enhances transparency and facilitates integration with other materials as a protective layer, overcoming existing fabrication limitations. Our research methodology involves reviewing previous literature and enhancing the mathematical modelling of current distribution. Notably, we consider current density changes in both X and Y directions, a novel approach. By modifying the edge of CA, we achieve greater bandwidth,

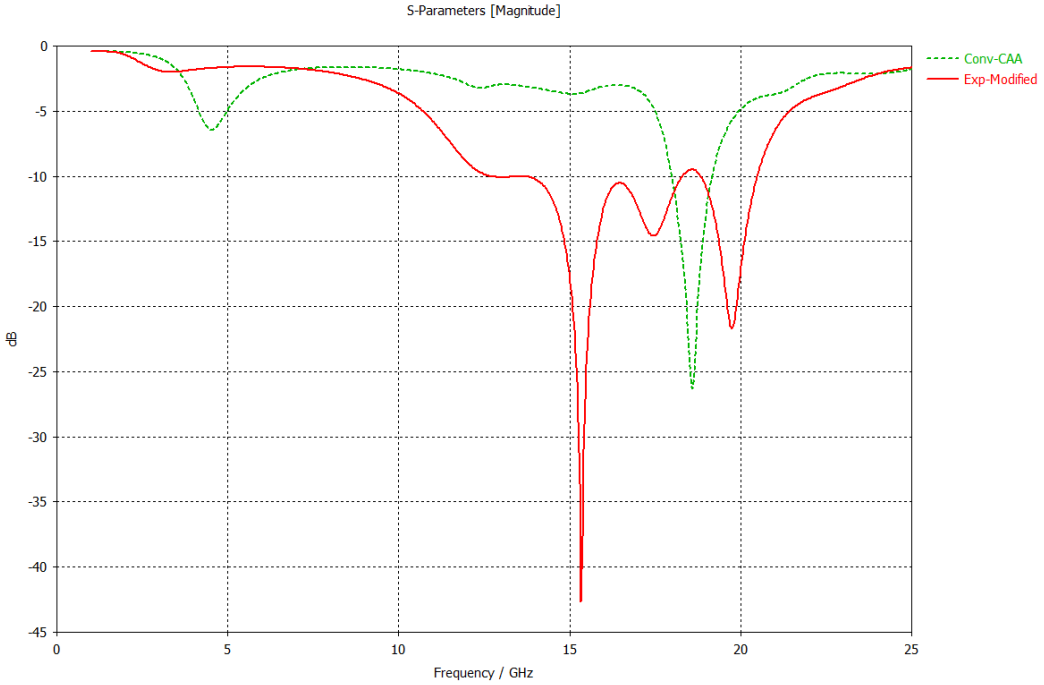

Fig. 8. Comparison of Conventional CAA With Respect to Exponentially Modified.

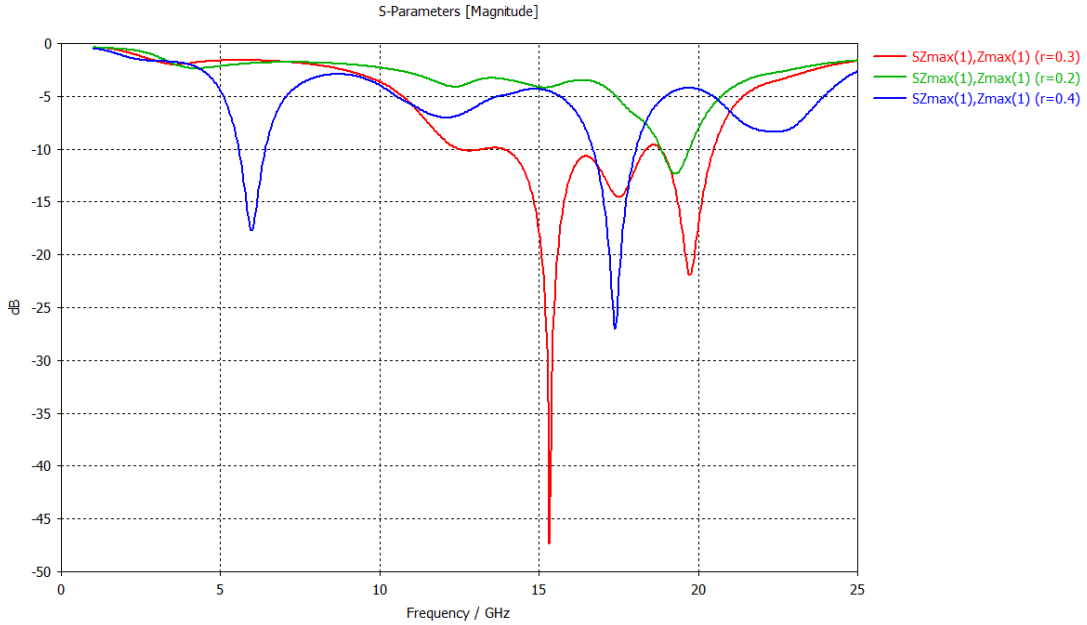

Fig. 9. Parametric Study of Exp-Modified CAA The Scattering Parameter Shows Variation with Regards to Exponentially rate r.

Table 1. Comparison review with previous research

Reference	Thickness	Number of layers	Bandwidth (GHz)	Relative Bandwidth	Substrate
[24]	0.103λ	1	5.6-19	85%	PVC
[25]	0.123λ	1	8-18	90%	PVC
[26]	0.08λ	1	6-16.5	90%	PVC
[27]	0.138λ	2	4.3-11.10	88%	PVC
[28]	0.06λ	3	1.98–18.6	167.4	PET
[29]	0.062λ	4	1.81–20.4	90%	PDMS
This work	0.139λ	1	12.5-21	85%	PVC

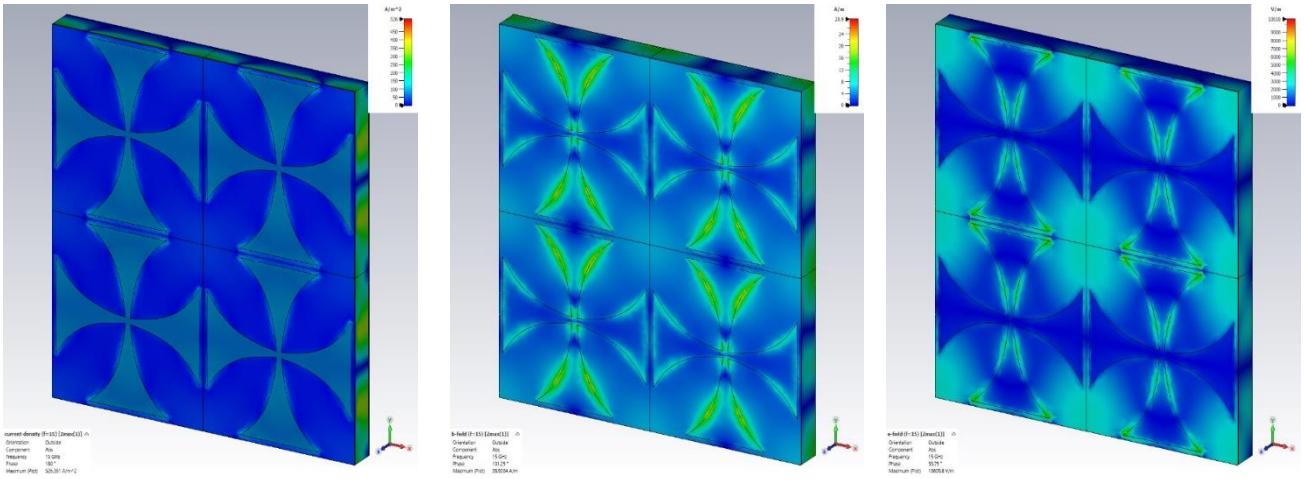

Fig. 10. Current Distribution at Frequency Of 15 At Different Phases

leading to the introduction of a new type of CAA.

3- 3- The Current Distribution

The current distribution in a CAA can vary depending on the design parameters and the operating frequency range. Overall, the current distribution in a CAA is complex and depends on the specific design parameters and operating frequency range. Understanding the current distribution is important for optimizing the absorption performance and designing CAAs for specific applications.

In the context of Circuit Analog Absorbers (CAA), when the metallic patch is operating at its resonance frequency, the current distribution on the patch is maximum, which indicates that the patch is acting as a short circuit. This means that the impedance of the patch at resonance is equal to zero, and thus the patch is highly conductive, allowing a maximum amount of current to flow through it. As a result, the incident electromagnetic waves are strongly reflected by the patch, which leads to a high absorption of the energy.

On the other hand, at frequencies away from the resonance frequency, the current distribution on the patch is non-uniform and concentrated near the slots. This indicates that the absorption is mainly due to the slot resonances, rather than the patch resonance. The slots on the metallic patch create a periodic structure that interacts with the incident waves to create resonances. These resonances can lead to constructive interference between the incident and reflected waves, resulting in a strong absorption of the energy.

Figure 10 shows the current density at the frequency of 15 Ghz with different phases. The current density at the

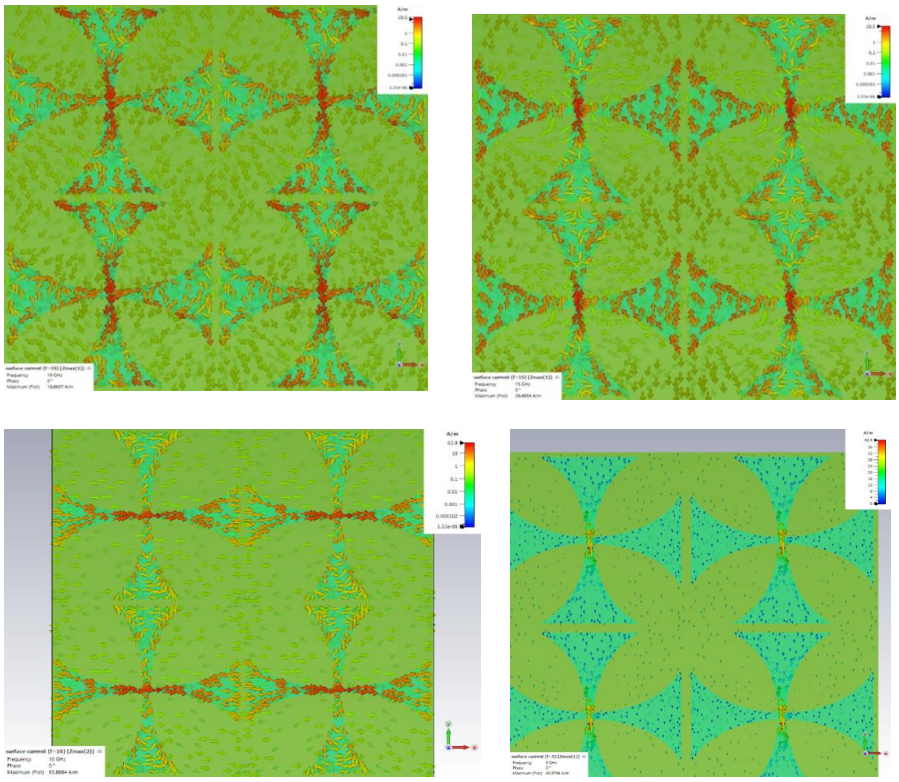

Fig. 11. Surface Current Distribution at Frequencies Of 5,10 15 And 19 GHz

exponential edge of the strip is maximum and shows that the absorption in this area is maximum at resonance frequency.

This current distribution can be explained mathematically with a Given a sinusoidal current distribution in both x and z directions for a periodic structure, the total current density J(x, z) can be expressed as a sum of Bloch waves:

$$J(x,z) = \sum_{m,n} C_{mn}.\sin\left(\frac{\pi x}{D_x}\right).\sin\left(\frac{\pi z}{D_z}\right).e^{-j\beta_m x}.e^{-j\beta_n z} \quad (17)$$

Here:

C_{mn} are coefficients representing the contribution of each mode.

D_x *and* D_z are the spacings between elements in the x and z directions, respectively.

β_m *and* β_n are the phase constants in the x and z directions for the m-th and n-th modes.

Now, let's substitute this into the power dissipation integral:

$$P = R\int_{\frac{-w}{2}e^z}^{\frac{w}{2}e^z}\int_{-l}^{l}\left|\sum_{m,n} C_{mn}.\sin\left(\frac{\pi x}{D_x}\right).\sin\left(\frac{\pi z}{D_z}\right).e^{-j\beta_m x}.e^{-j\beta_n z}\right|^2 d_x d_z \quad (18)$$

Now, let's proceed by expanding the square of the sum and simplifying the expression:

$$P = R\int_{\frac{-w}{2}e^z}^{\frac{w}{2}e^z}\int_{-l}^{l}\left|\sum_{m,n,p,q} C_{mn}C_{pq}^{*}.\sin^2\left(\frac{\pi x}{D_x}\right).\sin^2\left(\frac{\pi z}{D_z}\right).e^{-j(\beta_m-\beta_p)x}.e^{-j(\beta_n-\beta_q)z}\right|^2 d_x d_z \quad (19)$$

Now, let's integrate over x and z with the periodic functions:

$$P = R\sum_{m,n,p,q} C_{mn}C_{pq}^{*} .\int_{\frac{-w}{2}e^z}^{\frac{w}{2}e^z} e^{-j(\beta_m-\beta_p)x}d_z .\int_{-l}^{l} e^{-j(\beta_n-\beta_q)z}d_x \quad (20)$$

These integrals involve terms like Dirac delta functions and will enforce conditions for certain modes to contribute significantly to the integral. The specific values of the coefficients C_{mn}, the spacing and D_x *and* D_z, and other constants will influence the final form of the solution.

Also, surface currents at different frequencies such as 5,10,15 and 19 GHz are shown as Figure 11.

4- CONCLUSION

The novel design of an optically transparent circuit analogue absorber by modifying the exponentially tapered edge of the unit cell has been presented in this paper. By investigating various design parameters and types of circuit analogue elements, the absorber's impedance matching and absorption properties have been improved. The use of periodic structures and optimization of the absorber's dimensions have mitigated the fringing effect on orthogonal cross strips. The proposed design aims to achieve a balance between wide bandwidth electromagnetic shielding and high optical transparency, making it suitable for various applications in industries, medicine, and the military. The novel exponentially tapered design achieved a resonant frequency of 15.327 GHz with an absorption level of -42.67 dB. This performance significantly surpasses conventional designs, aligning with theoretical predictions and demonstrating practical applicability in areas requiring high optical transparency and wide bandwidth.

References

[1] B. A. Munk, Frequency Selective Surfaces: Theory and Design, John Wiley & Sons, Inc., 2003.

[2] A. Sohrab and Z. Atlasbaf, "A Circuit Analog Absorber With Optimum Thickness and Response in X-Band," IEEE Antennas and Wireless Propagation Letters, vol. 12, pp. 276-279, 2013.

[3] G. Van der plas, A. Barel and E. Schweicher, "A spectral iteration technique for analyzing scattering from circuit analog absorbers," IEEE Transactions on Antennas and Propagation, vol. 37, no. 10, pp. 1327-1332, Oct.1989.

[4] W.-H. Choi, J.-H. Shin, T.-H. Song, J.-B. Kim, C.-M. Cho, W.-J. Lee and C.-G. Kim, "Design of Circuit-Analog (CA) Absorber and Application to the Leading Edge of a Wing-Shaped Structure," IEEE Transactions on Electromagnetic Compatibility, vol. 56, no. 3, pp. 599-607, June-2014.

[5] E. Weber, Electromagnetic Fields, New York: Wiley, 1950, pp. 11 1-1 15 and p. 337.

[6] B. Munk, P. Munk and J. Pryor, "On Designing Jaumann and Circuit Analog Absorbers (CA Absorbers) for Oblique Angle of Incidence," IEEE Transactions on Antennas and Propagation, vol. 55, no. 1, pp. 186-193, Jan.2007.

[7] H. &. S. K. Mosallaei, "A one-layer ultra-thin meta-surface absorber.," 2005 IEEE Antennas and Propagation Society International Symposium, vol. 1, pp. 615-618, july-2005.

[8] B. Munk, R. Kouyoumjian and L. Peters, "Reflection properties of periodic surfaces of loaded dipoles," IEEE Transactions on Antennas and Propagation, vol. 19, no. 5, pp. 612-617, 1971.

[9] M. C. &. M. A. V. Hegg, "Influence of variable plate separation on fringing electric fields in parallel-plate capacitors," Conference record of the 2004 IEEE international symposium on electrical insulation, pp. 384-387, september-2004.

[10] C.-C. Chen, "Scattering by a two-dimensional periodic array of conducting plates," IEEE Transactions on Antennas and Propagation, vol. 18, no. 5, pp. 660-665, September,1970.

[11] Alwan, A. Elias, A. Kiourti and J. L. Volakis, "Indium tin oxide film characterization at 0.1–20 GHz using coaxial probe method," IEEE access 3, vol. 3, pp. 648-652, 2015.

[12] S. Barone, M. Narcowich and F. Narchowich, "Floquet theory and applications," Physical Review A, vol. 15, no. 3, p. 1109, 1077.

[13] P. A. Kuchment, Floquet theory for partial differential equations, vol. 60, Springer Science & Business Media, 1993.

[14] C. Chicone, Ordinary Differential Equations with Applications, New york: Springer New York, 2006.

[15] D. M. Kerns, Plane-wave scattering-matrix theory of antennas and antenna-antenna interactions, vol. 162, Department of Commerce, National Bureau of Standards, 1981.

[16] R. Hall, R. Mittra and K. Mitzner, "Analysis of multilayered periodic structures using generalized scattering matrix theory," IEEE Transactions on Antennas and Propagation, vol. 36, no. 4, pp. 511-517, April 1988.

[17] D. Systems, "simulia," CST Studio Suite, Electromagnetic field simulation software, 2023. [Online]. Available: https://www.3ds.com/products-services/simulia/products/cst-studio-suite/.

[18] F. Bloch, Zeitschrift fur Physik, vol. 52, pp. 555-600, 1928.

[19] R. Burleson, A. Terzuoli, E. English and L. Henderson, "Tapered periodic edge treatments for diffraction reduction," Seattle, WA, USA, 1994.

[20] G. Vendelin, A. Pavio, U. Rohde and M. Rudolph, Microwave circuit design using linear and nonlinear techniques, John Wiley & Sons, 2021.

[21] M. Steer, Microwave and RF Design III - Networks, North Carolina State University, 2019.

[22] A. Bayat and r. Mirzakhani, "A parametric study and design of the balanced antipodal Vivaldi antenna (BAVA)," PIERS Proceedings., vol. 19, 2012.

[23] G. Van der plas, A. Barel and E. Schweicher, "A spectral iteration technique for analyzing scattering from circuit analog absorbers," IEEE transactions on antennas and propagation, vol. 37, no. 10, pp. 1327-1332, 1989.

[24] H. Dawei, C. Jie, L. Wei, Z. Cheng and W. Tianlong, "Optically Transparent Broadband Microwave Absorption Metamaterial By Standing-Up Closed-Ring Resonators," Advanced Optical Materials, vol. 5, no. 13, p. 1700109, May 2017.

[25] Q. Zhou, X. Yin and F. e. a. Ye, "Optically transparent and flexible broadband microwave metamaterial absorber with sandwich structure," vol. 125, p. 131, 28 january

2019.

[26] R. Deng, K. Zhang, M. Li, L. Song and T. Zhang, "Targeted design, analysis and experimental characterization of flexible microwave absorber for window application," Materials & Design, vol. 162, pp. 119-129, 15 january 2019.

[27] H. Jiang, W. Yang, R. Li, S. Lei, B. Chen and H. Hu, "A conformal metamaterial-based optically transparent microwave absorber with high angular stability," IEEE Antennas Wireless Propagation Letter, vol. 20, no. 8, p. 1399–1403, Aug 2021.

[28] H. Jing, Y. Wei, J. Kang, C. Song, H. Deng, J. Duan, Z. Qu, J. Wang and B. Zhang, "An optically transparent flexible metasurface absorber with broadband radar absorption and low infrared emissivity," Journal of Physics D: Applied Physics, vol. 56, no. 11, p. 115103, 23 February 2023.

[29] Y. Gao, H. Jing, J. Wang, J. Kang, L. Zhao, L. Chen, Y. Wang, J. Duan, Z. Qu and B. Zhang, "A transparent broadband flexible metamaterial absorber for radar infrared-compatible stealth," Journal of Physics D: Applied Physics, vol. 57, no. 15, p. 155102, 22 January 2024.

[30] H. B. Palmer, "The capacitance of a parallel-plate capacitor by the Schwartz-Christoffel transformation," Electrical Engineering, vol. 56, no. 3, pp. 363-368, 1937.

[31] Sheokand, Harsh and et al, "An optically transparent broadband microwave absorber using interdigital capacitance," IEEE antennas and wireless propagation letters, vol. 18, no. 1, pp. 113-117, 2018.

[32] Pillai and K.P.P, "Fringing field of finite parallel-plate capacitors.," Proceedings of the Institution of Electrical Engineers . IET Digital Library, vol. 117, no. 6, pp. 1201-12-4, june-1970.

[33] Y. Li, P.-F. Gu, Z. He, Z. Cao, J. Cao, K. Wa Leung and D. Ding, "An Ultra-Wideband Multilayer Absorber Using an Equivalent Circuit-Based Approach," IEEE Transactions on Antennas and Propagation, vol. 70, no. 12, pp. 11911-11921, 2022.

[34] A. Rida, "Circuit analog absorber based on the Jerusalem cross," IEEE Transactions on Antennas and Propagation, vol. 59, no. 5, pp. 1582-1587, 2011.

[35] C. Dai, Z. Shi and X. Yi, "Floquet theorem with open systems and its applications," American Physical Society, vol. 93, no. 3, 2016.

[36] S. Xiao, S. A. Fernandes and A. Ostendorf, "Selective Patterning of ITO on flexible PET Substrate by 1064nm picosecond Laser," Physics Procedia, vol. 12, pp. 125-132, 2011.

HOW TO CITE THIS ARTICLE

R. Mirzakhani, A. R. Bayat, Novel Design of Optically Transparent Circuit Analog Absorber by Modifying of exponentially tapered edge of element to achieve wider Bandwidth, AUT J. Model. Simul., 56(1) (2024) 55-68.

DOI: 10.22060/miscj.2024.22964.5353